Desalination and Water Treatment
www.deswater.com

doi: 10.5004/dwt.2019.24812

172 (2019) 86–95
December

Use of commercial activated carbon for the purification of synthetic water polluted by a pharmaceutical product

M. Zamouche[a,*], L. Mouni[b], A. Ayachi[a], I. Merniz[a]

[a]*Laboratory of Engineering and Processes of Environment (LIPE), Faculty of Process Engineering, University of Constantine 3, Constantine 25000, Algeria, Tel. +213 555 83 87 45; email: zamouche_meriem@yahoo.fr (M. Zamouche)*
[b]*Laboratoire de Gestion et Valorisation des Ressources Naturelles et Assurance Qualité. Faculté SNVST, Université Akli Mohand Oulhadj, 10000 Bouira, Algeria, email: lotfimouni@gmail.com*

Received 2 February 2019; Accepted 26 August 2019

ABSTRACT

Nowadays, pharmaceutical compounds are often detected in surface water and groundwater. The potentiality of commercial activated carbon (CAC) for the removal of ketoprofen (KP) from aqueous solution was studied. The effects of various parameters such as pH, time, temperature, mixture speed, ionic strength, adsorbent mass and initial concentrations of KP were examined. Batch kinetics and isotherm adsorption experiments were performed to remove KP from aqueous solution. It was found that KP removal by CAC increased with the initial KP concentration. Temperature of solution and stirring speed showed no effect on KP adsorption. However, the amount of KP removal decreased with increase of the pH value and concentration of salt in the solution. The experimental isotherm data reveals the suitability and applicability of the Freundlich and Temkin isotherms model (R^2 = 0,99). Besides, the adsorption kinetic was fitted well with the pseudo-second-order model. The results revealed that the CAC was found to be very effective adsorbent for the elimination of KP from aqueous solution.

Keywords: Ketoprofen; Adsorption; Commercial activated carbon; Kinetic and isotherm studies; Non-steroidal anti-inflammatory drugs

1. Introduction

The presence of drug residues in aquatic environments was discerned in the 1980s [1,2]. The source of their existence in aquatic environments comes from pharmaceutical industries, hospital wastes and urban wastewater in complete excreted form in the urine and feces as products of metabolism or during the blind spill of unused drugs, to finish at wastewater treatment plants [3].

The degree of toxicity of the pharmaceutical compounds (PhC) has been tested on experimental organisms such as algae, daphnia magna and fish. According to US and European guidelines, acute toxicity is declared when the concentration of the active ingredient in the effluents is greater than 1 mg/L (US legislation) or 10 ng/L (European Medicines Agency) [3].

They can cause a potential impact on aquatic and terrestrial organisms so that they are getting more attention mainly in surface water. Therefore, it is necessary to understand the environmental behavior of these organic contaminants.

Among the various PhC the Ketoprofen (KP), a non-steroidal anti-inflammatory drug (NSAID) was selected. This pharmaceutical is widely used as an anti-inflammatory and antipyretic drug [4]. NSAID such as KP, diclofenac, naproxen and aspirin inhibit certain functions (including growth) in vertebrates (non-mammals) and invertebrates [5]. In this context, effective and efficient removal of KP from water is necessary.

* Corresponding author.

Presented at the 4th International Conference on Recycling and Reuse 2018 (R&R2018), 24–26 October 2018, Istanbul, Turkey

Conventional wastewater treatment plants, including activated sludge processes, do not eliminate completely pharmaceuticals products from wastewater: elimination rates range from less than 20% to more than 80% for some pharmaceuticals [1]. A typical example is given by Maude et al. [6] where the elimination rate was between 8% and 53%.

In addition to biological treatment, which has showed weakness for the elimination of PhC, we quote the different technologies that have been reported in the literature for the elimination of these contaminants, including ultrasonic irradiation, combined advanced oxidation processes such as sonophotocatalytic degradation in the presence of Fe^{3+} and TiO_2, electrochemical degradation, membrane technologies, membrane distillation, extraction using molecularly imprinted polymers, membrane distillation, photocatalysis, catalytic wet air oxidation; hybrid technologies adsorption on mesoporous silica and activated carbons, among others [4–7].

Adsorption is considered as competitive technic for removing PhC from aquatic environments due to the simplicity of design, its profitability and its low operating cost [8].

Despite the fact that several synthesized materials show PhC adsorption efficiency, activated carbon remains the most used material especially in the case of adsorption of specific adsorbates, as is the case of PhC. In the literature, few works have studied the adsorption of KP, unlike ibuprofen, where several articles have studied the elimination of this drug from aqueous solutions.

The adsorption of KP from aqueous solutions was tested by various adsorbents, carbon nanotubes (CNTs) and CNTs modified with ionic liquids were tested on the adsorption of KP and sulfamethoxazole (SMX) in the study of Lawal et al. [9]. Carbon nanospheres derived from cellulose, was prepared by Feng et al. [10] to eliminate KP, benzophenone and diphenylamine from queues solution. Other synthesized adsorbents have yielded impressive results for the adsorption of KP and other NSAIDs, such as polyvinylpyrrolidone-coated magnetite nanoparticles [11], Metal-organic framework (MIL-101), with or without modifications [8], PPhA adsorbent, designed using "acid catalyst" functionalization [12] and goethite to adsorb three typical NSAIDs (KP, naproxen and diclofenac) in column chromatography, batch experiments [13].

In this study, we are interested to the adsorption of KP from an aqueous solution by commercial activated carbon (CAC). The effects of temperature, pH of solution and initial KP concentration, stirred speed and time removal have been studied. The best fit equilibrium isotherms were determined by applying various adsorption isotherm models such as Langmuir, Freundlich and Temkin. Adsorption kinetic models were also used to analyze the kinetics and mechanism of KP adsorption on the CAC used. This fundamental study will prove helpful for subsequent application in designing an adsorbent for the treatment of KP-containing effluent.

2. Materials and methods

In this work, a CAC (Biochem Chemopharma, Georgia-USA) was used as an adsorbent. The CAC has an average diameter less than or equal to 125 μm, it was chosen as adsorbent because of its efficiency to adsorb different molecules. Before use, the CAC was dried at 105°C for 24 h to remove the adsorbed water and subsequently stored in a desiccator until for further use. KP is NSAID belongs to the propionic acid NSAID class; its name is 2-(3-benzoylphenyl) propionic acid [14]. Both enantiomers possess different biological activities [15]. KP is a nonselective cyclooxygenase inhibitor; it has analgesic, antipyretic and antiarthritic effect through inhibiting the prostaglandin and leukotriene synthesis. KP has very strong anti-inflammatory effect [14]. This compound has a very low solubility in water (51 mg/L at 22°C) [16].

The KP molecular properties are molar mass (254.28 g/mol), solubility in pure water (51 mg/L at 22°C) and pKa = 4.54 at 25°C (Fig. 1).

2.1. Analysis of KP

KP ($C_{16}H_{14}O_3$) was selected as the adsorbate species. A stock solution was prepared by dissolving 50 mg of KP in the form of powder in 1 L of distilled water. The suspension was stirred until the complete dissolution of the KP. Desired concentrations of KP were prepared from the stock solution. KP concentration was estimated spectrophotometrically by monitoring the absorbance at 261 nm using a UV–vis spectrophotometer (Shimadzu Mini 1601, Germany). pH was measured using a pH meter (JENWAY, Romania).

2.2. Characterization

The pH of zero charge (pH_{PZC}) of the CAC was determined by the so–called pH drift method as given by Nandi et al. [17]. This technique involves using of NaCl at 0.01 mol/L at different initial pHs ranging from 2 to 12; the pH was adjusted in addition of HCl and/or NaOH at 0.1 mol/L. A volume of 50 mL of each solution was contacted with (0.25 g) masses of CAC with stirring for 48 h and the final pHs were measured and plotted vs. the initial pHs. The pH_{PZC} was determined by the value for which the pH_{final} is equal to the $pH_{initial}$ (pH_{PZC} is the point where the $pH_{final} = pH_{initial}$).

The acidic and basic surface functional groups were determinate by the Boehm titration method [18].

Textural characterization of the CAC was carried out by N_2 adsorption at 77 K using Quanta chrome (USA) Nova Win instrument (version 11.03). The Brunauer–Emmett–Teller (BET) [19]. The pore size, pore volume were calculated using BET method. The mesopore and micropore size distributions were estimated based on Barrett–Joyner–Halenda and Horvath–Kawazoe theory respectively [20].

The Fourier-transform infrared (FTIR) spectra were obtained using a Spectrum GX spectrometer (Agilent technology Cary 600 spectrometer, USA) at a 4 cm^{-1} resolution. About 150 mg KBr disks containing approximately 2% of CAC samples was prepared shortly before recording the FTIR spectra on an FTIR spectrophotometer in the range from 400 to 4,000 cm^{-1} with 4 cm^{-1} resolution.

2.3. Batch adsorption

2.3.1. Batch equilibrium and kinetic studies

The batch adsorption experiments were carried out by contacting 0.25 g of CAC with 100 mL of KP solutions in the sealed 200 mL flasks. The suspensions were magnetically stirred at 300 rpm at room temperature (25°C) at pH 5.

Sample at a volume of 2.5 mL was taken out from the beaker at a specified time interval until the adsorption equilibrium was reached and filtered using Millipore filters (Germany) (0.22 μm). The recovered filtrate was immediately analyzed by spectrophotometer (Shimadzu Mini 1601, Germany) at the wavelength of 261 nm.

The adsorbed amount (mg/g) of KP on the CAC, q_t at any time t or q_e at equilibrium, was obtained with the mass-balance equation:

$$q_t = \frac{(C_0 - C_t)}{m} \times V \quad (1)$$

$$q_e = \frac{(C_0 - C_e)}{m} \times V \quad (2)$$

where C_0: the initial concentration of KP (mg/L); C_t: the concentration of KP at time t (mg/L); C_e: the concentration of KP at the equilibrium (mg/L); V: Volume of the solution (L); m: Dose of the adsorbent (g).

The percentage removal of KP (%) was calculated using the following equation:

$$E = \frac{(C_0 - C_t)}{C_0} \times 100 \quad (3)$$

2.3.2. Effects of variable parameters

The effects of different parameters such as adsorbent dose, pH of solution, ionic strength, temperature and agitation time were studied.

2.3.2.1. Effect of adsorbent dose

The effect of adsorbent amount KP removal efficiency was investigated on an 300 rpm shaker at 25°C by changing the adsorbent amount from 0.05 to 4 g/L at the constant pH 5 and the initial concentrations of KP is 10 mg/L.

2.3.2.2. Effect of pH

The effect of pH on the efficiency of KP removal was studied by changing the initial pH value from 2 to 12 using hydrochloric acid and sodium hydroxide at constant initial concentrations of KP being 10 mg/L, with the initial concentration of the adsorbent being 2.5 g/L at 25°C.

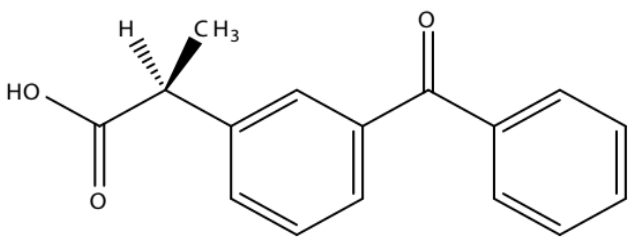

Fig. 1. Chemical structure of ketoprofen [15].

2.3.2.3. Effect of temperature

The temperature of solution is an important parameter for the establishment of the adsorption isotherms. To study the effect of this parameter we followed the variation of the adsorbed amount of drug as a function of time at different temperatures from 20°C to 50°C. The temperature was kept constant using water bath (Kottermann Labortechnik, Germany). The other parameters were fixed as 2.5 g/L (adsorbent dose/solution volume), stirred at 300°C, KP solution at concentration of 10 mg/L, solution volume of 0.1 L and without modifying pH.

2.3.2.4. Stirring rate

The effect of stirring rate on the removal of KP was evaluated by varying the speed stirring from 100 to 600 rpm with keeping the other parameters constants: pH 5 and the initial concentrations of KP, 10 mg/L, temperature of 25°C, KP solution at concentration of 10 mg/L.

2.3.2.5. Effect of salinity

Effect of salinity was studied by adding the NaCl (salt chosen) to the KP solution. The initial salt concentration was ranging from 50 to 300 mg/L. The other parameters were fixed as 2.5 g/L (adsorbent dose/solution volume), stirred at 300°C, KP solution at concentration of 10 mg/L, temperature of 25°C, solution volume of 0.1 L and without modifying pH.

3. Results and discussions

3.1. Characterization of CAC

The specific surface area (S_{BET}), average pore size by BET, and total pore volume of the CAC, as obtained from N_2 adsorption–desorption isotherms at 77 K, were 463.4 m^2/g, 27.36 Å and 0.13 cm^3/g, respectively.

As shown in Fig. 2, the pH_{PZC} of CAC was obtained by the intersection of the two curves is 7.1.

The results of Boehm titration (Table 1) show that the number of acidic functional groups is greater than that of the

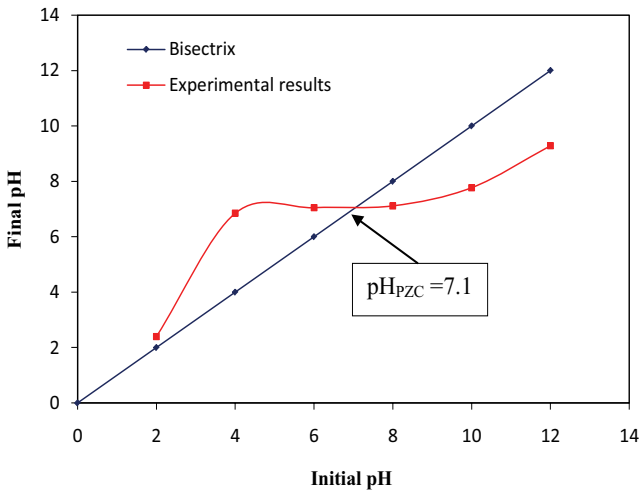

Fig. 2. Graphical representation of zero charge point pH_{PZC}.

Table 1
Concentration of functional groups of CAC

Concentration of functional groups	meq/g
Strong carboxylic acid (G I)	0.16
Lactone and weak carboxylic acid (G II)	0
Hydroxyl and phenol (G III)	0.55
Acidic functional groups	0.71
Basic functional groups	0

basic ones. The hydroxyl and phenol groups are predominant followed by the strong carboxylic acid groups, while the lactone and weak carboxylic acid groups are zero.

The FTIR technique is very useful for identification of the functional groups of the CAC solid. The surface functional groups of CAC were analyzed by the FTIR spectroscopy. The spectral range is 4,000–400 cm^{-1}. The FTIR spectrum revealed (Fig. 3) bands at about 3,030 cm^{-1} this band can be associated to –OH stretching vibration of hydroxyl functional groups. The peak at 3,300 cm^{-1} indicates the presence of the OH group, which can probably be attributed to adsorbed water on the carbon surface. The bands observed at about 2,950–2,850 cm^{-1} could be assigned to the aliphatic C–H group [21,22]. The peak at 2,760.87 (C=O) can be attributed to aldehyde groups. The spectra also displayed bands at 1,600 cm^{-1} corresponding to the C=C vibration in aromatic rings, and a peak at 1,240 cm^{-1} could be assigned to the stretching of C–O in esters, ethers or phenol groups.

3.2. Effect of adsorbent dose and contact time

To examine the effect of CAC dose on KP adsorption, the dose of adsorbent was varied from 0.05 to 4 g, while the initial KP concentration was kept constant (10 mg/L). Figs. 4a and b show that the amount of KP adsorbed decreases from 18.40 to 0.26 mg/g with the increase of the adsorbent dose, which is due to the increase in adsorbent surface area of the adsorbent.

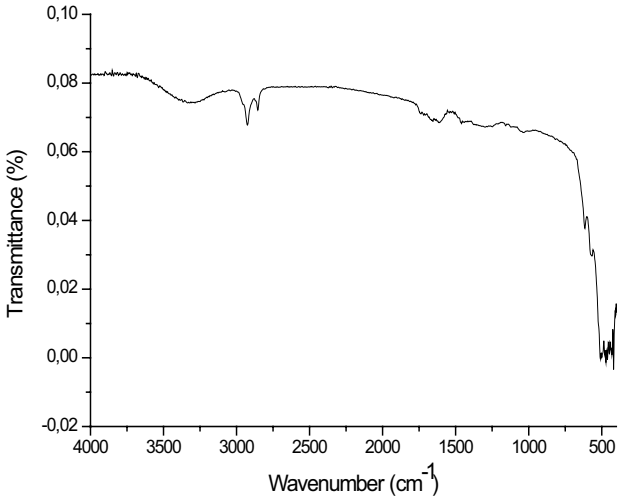

Fig. 3. FTIR spectra of CAC.

The maximum elimination (97.80%) was observed for a mass of 0.25 g, this adsorbent dose was selected as optimal. In addition, Fig. 4a shows rapid adsorption of KP from the first few minutes. The equilibrium conditions were reached at 5 min for all adsorbent doses studied which indicates the rapidity of adsorption process.

3.3. Effect of temperature

This parameter is important for the establishment of kinetic adsorption models, for which we have studied the percent of KP adsorbed as a function of temperatures from 20°C to 50°C, the results obtained are shown in Fig. 5. This figure shows that the amount of KP adsorbed is similar for all temperatures (≈94%) with an exception at the temperature of 25°C. At this temperature, a slight increase was observed in the percent of KP adsorbed (97.02%). Overall, the percentage removal decreased from 97.02% to 94.51% with increasing temperature from 25°C to 50°C respectively. This can be explained by the exothermicity of the adsorption process and the weakening of the bonds between KP

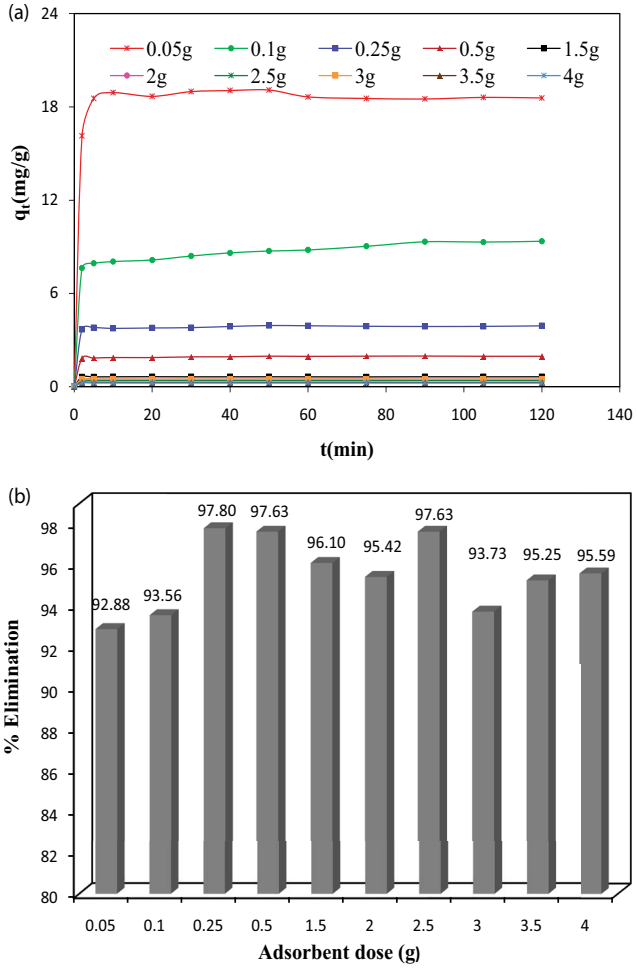

Fig. 4. (a) Effect of adsorbent dose on the elimination of ketoprofen (C_0 = 10 mg/L, W = 300 rpm, T = 25°C and pH = 5) and (b) Ketoprofen elimination percentage us function of adsorbent dose (C_0 = 10 mg/L, W = 300 rpm, T = 25°C and pH = 5).

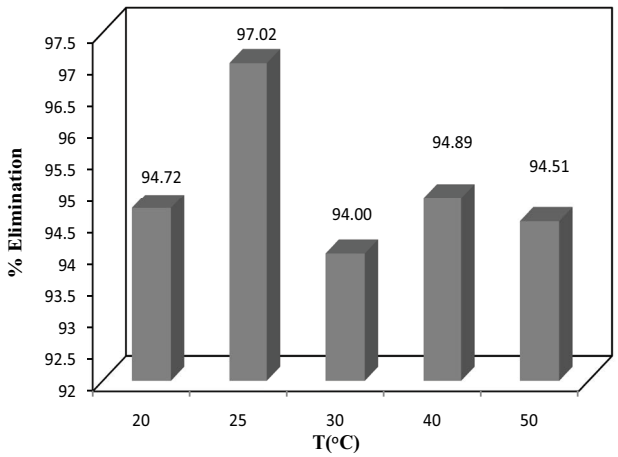

Fig. 5. Ketoprofen elimination percentage as function of the solution temperature (C_0 = 10 mg/L, m = 0.25 g, W = 300 rpm and pH = 5).

and adsorbent active sites for the highest temperatures. This result has been previously reported by Cuerda-Correa et al. [23], when studying the adsorption of KP and naproxen onto the carbon black BC-1300. They have reported also that as temperature raises the interaction occurring between the adsorbate and the active sites of the adsorbent become weaker, which is indicative of a physisorption process. Furthermore, an increase of temperature generally involves an increase of the solubility of the solute, thus favoring the adsorbate–adsorbent interaction forces and consequently decreases in adsorption [23]. The temperature of 25°C gives a very high percentage of elimination of KP, so this value is considered us an optimal value.

3.4. Effect of pH

The effect of pH solution is an important parameter on the amount of KP adsorbed by CAC. The initial pH of the solution pH was varied from 2 to 12; the latter is adjusted by the addition of hydrochloric acid (0.1 N) or sodium hydroxide (0.1 N). The concentration of KP (10 mg/L), solution temperature (25°C) and agitation speed (300 rpm) were kept constant. The effect of pH on the removal of KP by CAC is shown in Fig. 6.

As seen from the result obtained, the pH of solution has not a remarkable effect on the amount of KP adsorbed. At natural pH (without modification, pH = 5), a highly amount of KP was obtained (3.75 mg/g). At pH higher than 5, the amount adsorbed is slightly decreased from 3.67 to reach a value of 3.57 mg/g at pH 12. This result agrees with that found in the research paper Cuerda-Correa et al. [23], where the amount of KP adsorbed has decreased at neutral or basic pH values between 7 and 11. These variations with pH suggest that at this pH range the dissociation degree of the surface groups of the adsorbent (pH > pH_{PZC} = 7.1) as well as that of KP is high and both, the adsorbent and the adsorbate occur in their negatively charged forms, which induces electrostatic repulsions between the KP and the surface of the adsorbent [23]. At pH equal to 2, the adsorption capacity was more or less high (3.71 mg/g) and

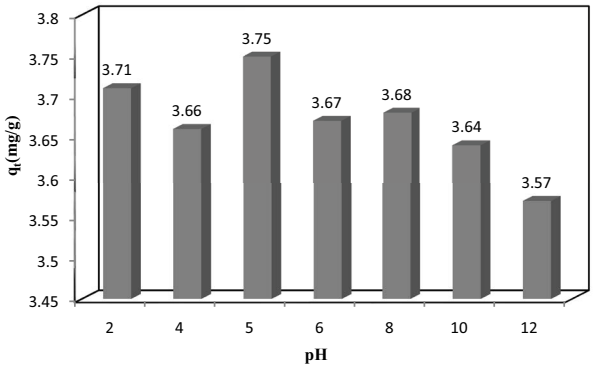

Fig. 6. Percentage removal of KP as function of the pH of the solution (C_0 = 10 mg/L, m = 0.25 g, W = 300 rpm and T = 25°C).

maximum at natural pH (pH = 5). At pH = 5, the activated carbon surface is positively charged (pH < pH_{pzc} = 7.1) and KP is always anionic, which causes an attraction between the drug and the activated carbon surface. The rises of the amount of KP adsorbed at low pH was also detected in the research of Cuerda-Correa et al. [23]. It was reported that the decrease of pH results in a noticeable decrease of the effective size of the KP molecule due to a decrease in the size of the hydration sphere, which would favor the access of the KP molecules into the porous texture of the adsorbent and, consequently, the adsorption of the KP. KP adsorption was also more favored at lower pH compared to other states in the study of Lawal et al. [9].

The optimal pH for the adsorption of KP with the CAC is the naturel pH of 5, the higher amount observed at this pH it was contributed to the physisorption since both the adsorbent and the solutes may be considered to be in their neutral or slightly dissociated forms as given in the Cuerda-Correa et al. [23].

3.5. Effect of stirring speed

The effect of stirring rate on the amount of KP adsorbed was determined from 100–600 rpm. As shown in Fig. 7 it was observed that there is no considerable change in the adsorption capacity of the CAC for the different speeds tested. The percent removal of KP was almost 93% for the 100, 500 and 600 rpm speeds. A slight decrease in the percent removal (≈92%), was observed for the two speeds 200 and 400 rpm. The decrease of percent removal at 200 rpm can be explained by the fact that this speed does not ensure a homogenization of the solution, and a good contact between the adsorbate and the adsorbent. The stirring speed has the effect of reducing the thickness of the liquid film which surrounds the particle and which constitutes a resistance to the transfer of matter [24]. This lets us predict that at the speed, the thickness of the boundary layer is not yet reduced, so it delays a little the mass transfer. The optimal stirring speed that gives the maximum KP elimination is equal to 300 rpm.

3.6. Effect of ionic strength

The ionic strength of the solution is one of the factors that controls both electrostatic and non-electrostatic

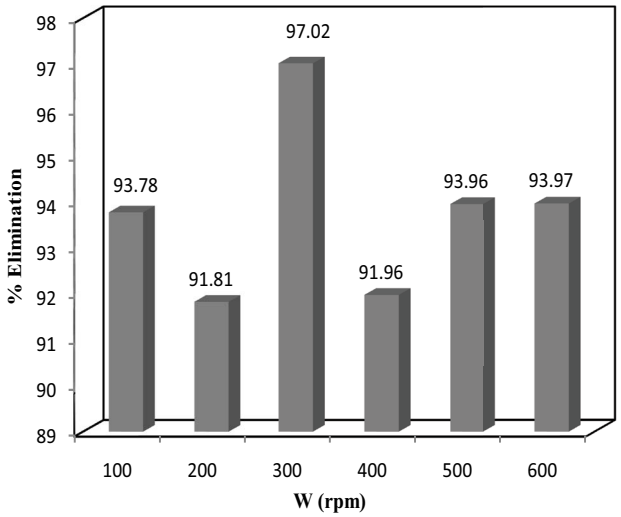

Fig. 7. Percent removal of KP as a function of the stirring speed (C_0 = 10 mg/L, m = 0.25 g, T = 25°C and $pH_{naturel}$ = 5).

interactions between the adsorbate and the adsorbent surface. The effect of salinity on the adsorption of KP by CAC was tested by using a NaCl at different initial concentrations ranging from 50 to 300 mg/L. As shown in Fig. 8, we observe that the presence of salt in the solution influences slightly the adsorption of KP by activated carbon, the adsorption capacity has slightly decreased from 3.64 to 3.46 mg/g when concentration of salt increased from 50 to 300 mg/L, respectively. This is probably due to the competition between the selected salt and the KP to occupy the active sites on the powder activated carbon surface. The presence of ionic strength generally influence negatively the adsorption since of strong competition effect between Na^+ and adsorbate to occupy the free sites on the adsorbent as motioned in the research of Pan et al. [25] and Niu et al. [26].

3.7. Effect of initial adsorbate concentration

To study the effect of the initial concentration of KP on adsorption by CAC varied the adsorbate concentration ranging from 2 to 20 mg/L. This effect was studied for both temperatures of 25°C and 35°C. According to the results obtained (Figs. 9 and 10) it is showed that when the initial concentration of KP increases from 2 to 20 mg/L the amount of KP adsorbed increases from 0.83 to 7.65 mg/g for the temperature of 25°C and from 0.6 to 7.44 mg/g for the temperature of 35°C respectively. This is due to an increase in driving force with the increase in the initial concentration of KP, since concentration provides driving force to overcome mass transfer resistance between solid and solution phases [27].

3.8. Isotherm experiments

Adsorption isotherm is the plot of adsorption uptake q_e (mg/g) and the final equilibrium solute concentration C_e (mg/L) at a given temperature adsorption [28]. The adsorption isotherm of KP by CAC was done at the temperature of 25°C. The behavior of the adsorption isotherms obtained

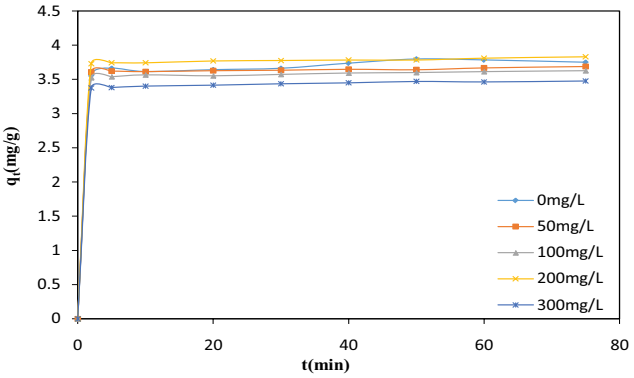

Fig. 8. Effect of the ionic strength (NaCl) on the adsorption of KP by CAC at different concentrations of salt (C_0 = 10 mg/L, m = 0.25 g, W = 300 rpm, T = 25°C and $pH_{naturel}$ = 5).

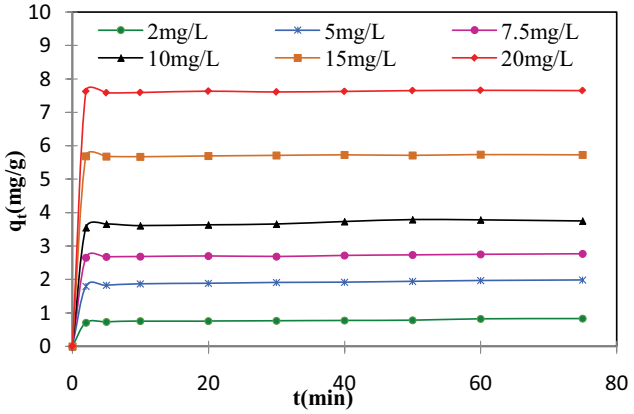

Fig. 9. Initial adsorbate concentration effect on the elimination of KP (C_0 = 2–20 mg/L, W = 300 rpm, m = 0.25 g, T = 25°C and $pH_{naturel}$ = 5).

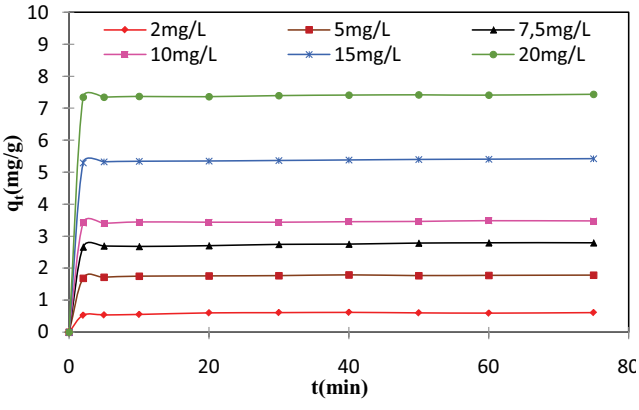

Fig. 10. Initial adsorbate concentration effect on the elimination of KP (C_0 = 2–20 mg/L, W = 300 rpm, m = 0.2 5 g, T = 35°C and $pH_{naturel}$ = 5).

(Fig. 11) shows that they can be classified according to the classification of Giles et al. [29]. By referring to this classification, the isotherm adsorption of KP on CAC was classified at an L-type (Langmuir) but at low concentrations [29]. The saturation of active sites in the adsorbent which

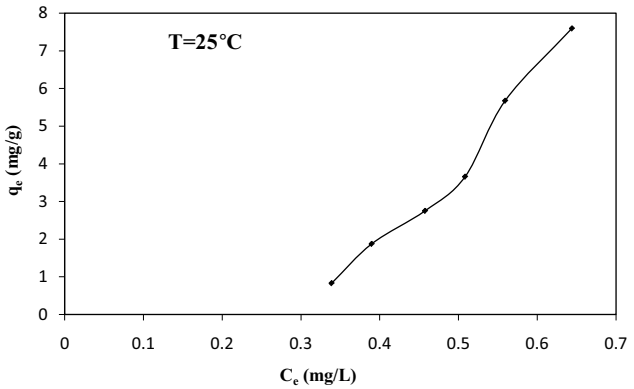

Fig. 11. Isotherm adsorption of KP by CAC at T = 25°C, t = 5 min, $pH_{naturel}$ = 5, dosage of 0.25 g/100 mL.

produce the formation of monolayer is not yet occurred due to the low concentration range studied (2–20 mg/L).

3.9. Modeling of equilibrium data by Langmuir, Freundlich and Temkin models

Adsorption isotherms were obtained from batch experiments at a temperature of 25°C (Table 2). The aim of these batch experiments was to obtain the maximum adsorption capacity (surface coverage). Based on this type of isotherm, Freundlich, Temkin, Langmuir and Sips models were used to fit the experimental curves. Table 2 shows the parameters of each model used for the adsorption of KP on CAC. The values of R^2 demonstrated that the Sips model could represent satisfactorily the adsorption equilibrium of KP on CAC.

The isotherm data for KP adsorption by CAC was not correctly fitted with Langmuir model as shown in Table 2 (R^2 = 0.244).

The Freundlich and Temkin models give a better fit of the experimental data followed by Sips model. This result is in agreement with the previously obtained result of adsorption isotherm curve at T 25°C, where the rate showed an increase in the adsorption capacity at equilibrium with the increase of the concentration (for low concentrations). This is in agreement with the Freundlich theory, which announces that the Freundlich isotherm equation is exponential it can only be reasonably applied in the low to intermediate concentration ranges [33]. This result is similar to that of Razanajatovo et al. [35] studies found that the experimental adsorption data of the pharmaceuticals product antibiotic SMX, beta-blocker propranolol and antidepressant sertraline on ultra-high molecular weight polyethylene microplastics were better adapted to the Freundlich model. The value of n (0.38) obtained from ranges between 0 and 1, that means a high surface heterogeneity or a high adsorption intensity and it becoming more heterogeneous as its value gets closer to zero [35]. The adsorption of KP on the CAC is probably a chemisorption's process, because and as reported in [35,36], if the value of n is below unity implies chemisorption's process. Freundlich isotherm is widely applied in heterogeneous systems especially for organic compounds or highly interactive species on activated carbon [35]. This is the reason that Freundlich isotherm was more adapted to our equilibrium results of adsorption of KP on CAC.

4. Kinetics study

Kinetics of adsorption of KP onto CAC was modelled by pseudo-first-order and pseudo-second-order kinetic equations (Table 3).The pseudo-first-order rate constant K_1 and q_e can be determined from slope and intercept of the graph by plotting log ($q_e - q_t$) vs. t (Fig. 12). While, the pseudo-second-order rate constant K_2 and q_e can be determined from slope and intercept of the graph by plotting t/q vs. t (Fig. 13). The calculated constants and R^2 values for the selected kinetic models were given in Table 3.

The pseudo-second-order model provided much better correlation coefficients (R^2) than pseudo-first-order model, As shown in Table 3, pseudo-second-order model provide better correlation coefficients than pseudo-first-order model,

Table 2
Isotherms parameters for removal of KP on CAC

Isotherms	Non-linear forms	Parameter	Value	SSE
Langmuir [30]	$\frac{q_e}{q_m} = \frac{KC_e}{1+KC_e}$	q_m (mg/g) K (L/g) R^2	18 0.8 0.244	13.44
Freundlich [30]	$q_e = K_F C_e^{\frac{1}{n}}$	K_F (L/g) n R^2	26.6 0.38 0.995	1.36
Temkin [31]	$\ln q_e = \frac{RT}{b}\ln\left(AC_e\right)$	A (L/g) B (J/mol) R^2	2,73 650 0,999	0.43
Sips [32]	$q_e = \frac{q_{ms}\left(K_s C_e\right)^{n_s}}{1+\left(K_s C_e\right)^{n_s}}$	q_{ms} K_s n_s R^2	9.1 1.7 2.9 0.96	1.48

Table 3
Comparison of the pseudo-first-order, pseudo-second-order adsorption rate constant and calculated and experimental q_e value obtained at different initial KP concentrations

Kinetics	Equations	Parameters	C_0 (mg/L)					
			2	5	7.5	10	15	20
Pseudo-first-order [9]	$\frac{dq_t}{dt} = K_1(q_e - q_t)$ and $\ln(q_e - q_t) = \ln q_e - K_1 t$	K_1	0.169	0.048	0.060	0.083	0.136	0.024
		$q_{e,\text{the}}$ (mg/g)	1.512	0.359	0.253	0.503	0.382	0.163
		$q_{e,\text{exp}}$ (mg/g)	0.832	1.991	2.753	3.749	5.737	7.662
		R^2	0.522	0.679	0.516	0.568	0.338	0.096
Pseudo-second-order [36]	$\frac{dq}{dt} = K_2(q_e - q_t)^2$ and $\frac{t}{q_t} = \frac{1}{K_2 q_e^2} + \frac{t}{q_e}$	K_2	0.887	0.658	0.951	0.652	2.17	1.815
		$q_{e,\text{the}}$ (mg/g)	0.831	1.992	2.770	3.784	5.737	7.657
		$q_{e,\text{exp}}$ (mg/g)	0.832	1.991	2.773	3.749	5.731	7.649
		R^2	0.998	0.999	0.999	0.999	1	1

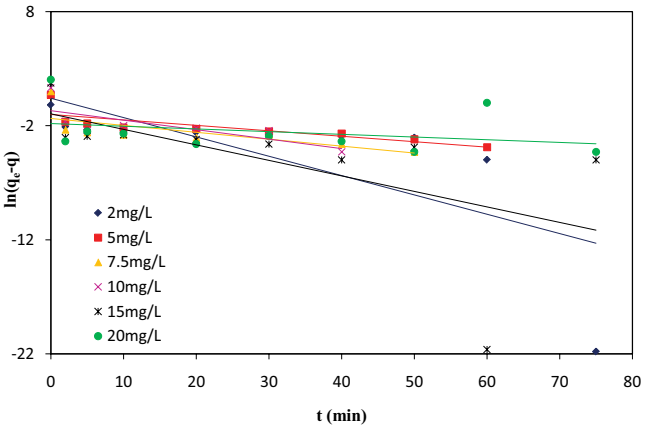

Fig. 12. Plot of the linear form of the pseudo-first-order kinetic model at T = 25°C.

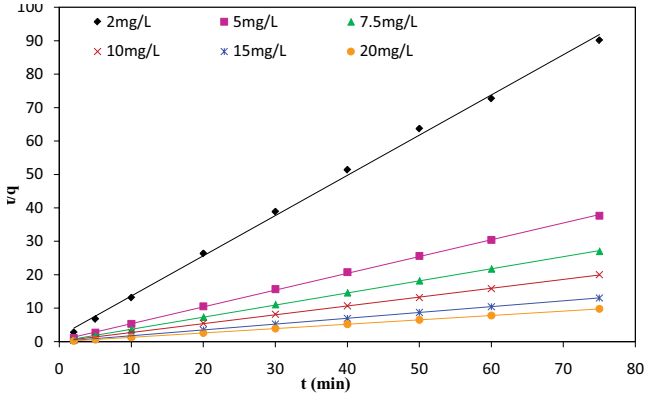

Fig. 13. Plot of the linear form of the pseudo-second-order kinetic model at T = 25°C.

and we can conclude that pseudo-second-order model is more suitable to explain the adsorption kinetics mechanism.

The intraparticle diffusion model based on the theory proposed by Weber and Morris (Table 4) was tested to identify the diffusion mechanism. The results shown in Fig. 14

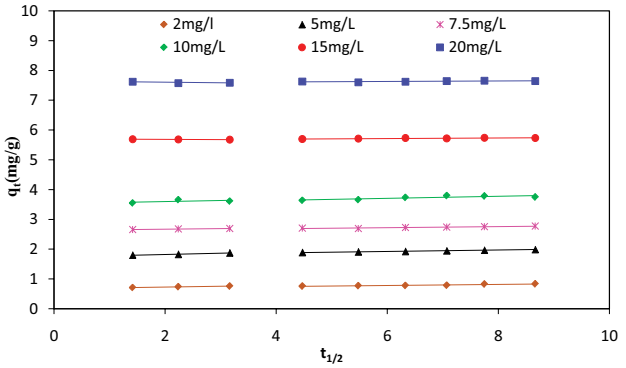

Fig. 14. Plots of KP adsorption onto CAC by intraparticle diffusion model at 25°C.

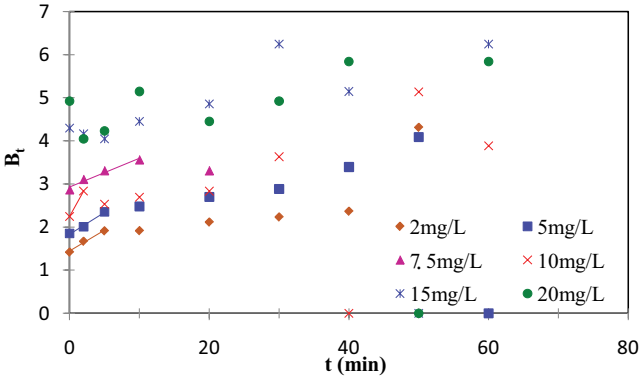

Fig. 15. Plots of KP adsorption onto CAC by Boyd model at 25°C.

and those recorded in Table 4 show that the correlation coefficients are unsatisfactory. For intraparticle diffusion plots, the lines obtained do not pass through the origin, they are multilinear containing two segments, and the first region at all concentrations indicates that the diffusion in the pores does not control the overall rate of adsorption. Therefore, it is confirmed that the first linear segments represent the diffusion in the film and that the second

Table 4
Intraparticle diffusion constants for different initial KP concentrations

Intraparticle diffusion [36]	$q_t = K_i t^{\frac{1}{2}} + C_d$	K_1 (mg/g min$^{1/2}$)	0.027	0.043	0.019	0.033	–0.007	–0.02
		C_1 (mg/g)	0.674	1.738	2.632	3.534	5.701	7.644
		R_1^2	0.986	0.985	0.978	0.283	0.999	0.446
		K_2 (mg/g min$^{1/2}$)	0.019	0.025	0.019	0.034	0.008	0.008
		C_2 (mg/g)	0.668	1.773	2.609	3.501	5.665	7.583
		R_2^2	0.889	0.986	0.880	0.668	0.702	0.447
Boyd [39]	$F = 1 - \frac{6}{\pi^2}\exp(-B_t)$ and B_t = –0.4977–ln (1–F) and $F = q/q_e$							

linear segments represent the intraparticle diffusion into the porous structure CAC [37]. Overall, the increase in the initial KP concentration results in an increase in the calculated *y*-intercept value for all concentrations studied. This indicates that the intra-particle diffusion is less and less involved in the adsorption process, the ordinate at the origin informs about the effect of the boundary layer, the greater it is the more the contribution of the external diffusion in limitation of the adsorption rate is important [36,38,39].

From Fig. 15, the evolution of Bt (Boyd model) as a function of time for different initial concentrations at T = 25°C show that linear segments are obtained only for the initial period for all studied concentrations, indicating that the external mass transfer is the adsorption limiting process only at the beginning first 5 min [38].

5. Conclusion

The adsorption of KP from aqueous solution using CAC as adsorbent was investigated in batch process. The process variables were optimized and maximum KP percent removal (97.02%) was reached at 2.5 g adsorbent dose, temperature of 25°C pH 5, stirring speed of 300 rpm and KP initial concentration of 10 mg/L. Ionic strength was found to have an influence on the adsorption efficiency. The Freundlich and Temkin adsorption isotherms were found to have the best fit to the experimental data with a correlation coefficient R^2 equal to 0.995 and 0.999 respectively. The value of n (0.38) obtained indicate a high surface heterogeneity. The KP maximum adsorption capacity (Q_{max}) estimated from the Sips isotherm model was 9.1 mg/g.

The adsorption kinetics can be predicted by pseudo-second-order kinetic. The intraparticle diffusion kinetic model was not the main mechanism involved in the adsorption of KP. Thus, CAC can be used as a good material to uptake pharmaceuticals from aqueous solution.

References

[1] D. Musmarra, M. Prisciandaro, M. Capocelli, D. Karatza, P. Iovino, S. Canzano, A. Lancia, Degradation of ibuprofen by hydrodynamic cavitation: reaction pathways and effect of operational parameters, Ultrason. Sonochem., 29 (2016) 76–83.
[2] T.M. Defarges, M. Guerbet, J. Massol, Impact des médicaments sur l'environnement: état des lieux, évaluation des risques, communication, Thérapies, 66 (2011) 335–340.
[3] P. Banerjee, P. Das, A. Zaman, P. Das, Application of graphene oxide nanoplatelets for adsorption of Ibuprofen from aqueous solutions: evaluation of process kinetics and thermodynamics, Process Saf. Environ. Prot., 101 (2016) 45–53.
[4] D. Bahamon, L. Carro, S. Guri, L.F. Vega, Computational study of ibuprofen removal from water by adsorption in realistic activated carbons, J. Colloid Interface Sci., 498 (2017) 323–334.
[5] F.A. Velichkova, Vers un procède Fenton Hétérogène pour le traitement en continu d'eau polluée par des polluants pharmaceutiques, Thèse de doctorat. Institut National Polytechnique de Toulouse (INP Toulouse), 20 Janvier 2014.
[6] C.-B. Maude, J. Alice, M. Catherine, B. Gilles, Contamination des milieux aquatiques par les substances pharmaceutiques et cosmétiques - Etat des lieux et perspectives, R.INT.DCN. BE.ARC/2009.01, 2009.
[7] S. Álvarez-Torrellas, A. Rodríguez, G. Ovejero, J. García, Comparative adsorption performance of ibuprofen and tetracycline from aqueous solution by carbonaceous materials, Chem. Eng. J., 283 (2016) 936–947.
[8] J.Y. Song, S.H. Jhung, Adsorption of pharmaceuticals and personal care products over metal-organic frameworks functionalized with hydroxyl groups: quantitative analyses of H-bonding in adsorption, Chem. Eng. J., 322 (2017) 366–374.
[9] I.A. Lawal, M.M. Lawal, S.O. Akpotu, M.A. Azeez, P. Ndungu, B. Moodley, Theoretical and experimental adsorption studies of sulfamethoxazole and ketoprofen on synthesized ionic liquids modified CNTs, Ecotoxicol. Environ. Saf., 161 (2018) 542–552.
[10] Z.X. Feng, K. Odelius, G.K. Rajarao, M. Hakkarainen, Microwave carbonized cellulose for trace pharmaceutical adsorption, Chem. Eng. J., 346 (2018) 557–566.
[11] M.A. Fard, A. Vosoogh, B. Barkdoll, B. Aminzadeh, Using polymer coated nanoparticles for adsorption of micropollutants from water, Colloids Surf., A, 531 (2017) 189–197
[12] M.T. Sekulic, N. Boskovic, A. Slavkovic, J. Garunovic, S. Kolakovic, S. Pap, Surface functionalised adsorbent for emerging pharmaceutical removal: adsorption performance and mechanisms, Process Saf. Environ. Prot., 125 (2019) 50–63.
[13] C.L. Yu, J. Bahashi, E.P. Bi, Mechanisms and quantification of adsorption of three anti-inflammatory pharmaceuticals onto goethite with/without surface-bound organic acids, Chemosphere, 222 (2019) 593–602.
[14] A. Abd-Elbary, M.A. El Nabarawi, D.H. Hassen, A.A. Taha, Inclusion and characterization of ketoprofen into different mesoporous silica nanoparticles using three loading methods, Int. J. Pharm. Pharm. Sci., 6 (2014) 183–191.
[15] S. Rençber, S.Y. Karavana, M. Özyazici, Bioavailability file: ketoprofen, Pharm. Sci., 34 (2009) 203–216.
[16] Y. Gao, M.A. Deshusses, Adsorption of clofibric acid and ketoprofen onto powdered activated carbon: effect of natural organic matter, Environ. Technol., 33 (2011) 1719–1727.
[17] B.K. Nandi, A. Goswami, M.K. Purkait, Adsorption characteristics of brilliant green dye on kaolin, J. Hazard. Mater., 161 (2009) 387–395.
[18] H.P. Boehm, Chemical identification of surface groups, Adv. Catal., 16 (1966) 179–274.
[19] F. Rouquerol, J. Rouquerol, K. Sing, Adsorption by Powders and Porous Solids: Principles, Methodology and Applications, Academic Press, San Diego, CA, 1999.

[20] S. Storck, H. Bretinger, W.F. Maier, Characterization of micro- and mesoporous solids by physisorption methods and pore-size analysis, Appl. Catal., A, 174 (1998) 137–146.
[21] N. Bouchelkia, L. Mouni, L. Belkhiri, A. Bouzaza, J.-C. Bollinger, K. Madani, F. Dahmoune, Removal of lead(II) from water using activated carbon developed from jujube stones, a low-cost sorbent, Sep. Sci. Technol., 51 (2016) 1645–1653.
[22] Md. Tamez Uddin, Md. Akhtarul Islam, S. Mahmud, Md. Rukanuzzaman, Adsorptive removal of methylene blue by tea waste, J. Hazard. Mater., 164 (2009) 53–60.
[23] E.M. Cuerda-Correa, J.R. Domínguez-Vargas, F.J. Olivares-Marín, J.B. de Heredia, On the use of carbon blacks as potential low-cost adsorbents for the removal of non-steroidal anti-inflammatory drugs from river water, J. Hazard. Mater., 177 (2010) 1046–1053.
[24] El-Khamsa Guechi, O. Hamdaoui, Sorption of malachite green from aqueous solution by potato peel: kinetics and equilibrium modeling using non-linear analysis method, Arabian J. Chem., 9 (2016) 416–424.
[25] D.-q. Pan, Q.-h. Fan, P. Li, S.-p. Liu, W.-s. Wu, Sorption of Th(IV) on Na-bentonite: effects of pH, ionic strength, humic substances and temperature, Chem. Eng. J., 172 (2011) 898–905.
[26] Z.W. Niu, Q.H. Fan, W.H. Wang, J.Z. Xu, L. Chen, W.S. Wu, Effect of pH, ionic strength and humic acid on the sorption of uranium(VI) to attapulgite, Appl. Radiat. Isot., 67 (2009) 1582–1590.
[27] S. Shoukat, H.N. Bhatti, M. Iqbal, S. Noreen, Mango stone biocomposite preparation and application for crystal violet adsorption: a mechanistic study, Microporous Mesoporous Mater., 239 (2017) 180–189.
[28] K. Vijayaraghavan, T.V.N. Padmesh, K. Palanivelu, M. Velan, Biosorption of nickel(II) ions onto *Sargassum wightii*: application of two-parameter and three-parameter isotherm models, J. Hazard. Mater., 133 (2006) 304–308.
[29] C.H. Giles, T.H. MacEwan, S.N. Nakhwa, D. Smithm, Studies in adsorption., Part XI. A system of classification of solution adsorption isotherms and its use in diagnosis of adsorption mechanisms and in measurement of specific surface areas of solids, J. Chem. Soc., 10 (1960) 3973–3993.
[30] O. Hamdaoui, E. Naffrechoux, Modeling of adsorption isotherms of phenol and chlorophenols onto granular activated carbon: Part I. Two-parameter models and equations allowing determination of thermodynamic parameters, J. Hazard. Mater., 147 (2007) 381–394.
[31] B.H. Hameed, Evaluation of papaya seeds as a novel non-conventional low-cost adsorbent for removal of methylene blue, J. Hazard. Mater., 162 (2009) 939–944.
[32] N.T.R.N. Kumara, N. Hamdan, M.I. Petra, K.U. Tennakoon, P. Ekanayake, Equilibrium isotherm studies of adsorption of pigments extracted from kuduk-kuduk (*Melastoma malabathricum* L.) pulp onto TiO_2 nanoparticles, J. Chem., 2014 (2014) 6 p.
[33] Y. Liu, Y.-J. Liu, Biosorption isotherms, kinetics and thermodynamics, Sep. Purif. Technol., 61 (2008) 229–242.
[34] R.M. Razanajatovo, J.N. Ding, S.S. Zhang, H. Jiang, H. Zou, Sorption and desorption of selected pharmaceuticals by polyethylene microplastics, Mar. Pollut. Bull., 136 (2018) 516–523.
[35] K.Y. Foo, B.H. Hameed, Insights into the modeling of adsorption isotherm systems, Chem. Eng. J., 156 (2010) 2–10.
[36] B.H. Hameed, Spent tea leaves: a new non-conventional and low-cost adsorbent for removal of basic dye from aqueous solutions, J. Hazard. Mater., 161 (2009) 753–759.
[37] D. Suteu, C. Zaharia, M. Badeanu, Kinetic modeling of dye sorption from aqueous solutions onto apple seed powder, Cellul. Chem. Technol., 50 (2016) 1085–1091.
[38] S.A. Zulkepli, Md.P. Abdullah, W.M.A.W.M. Khalik, Removal of malachite green dye from aqueous solution using multi-walled carbon nanotubes: an application of experimental design, Malaysian J. Anal. Sci., 20 (2016) 258–271.
[39] B.H. Hameed, M.I. El-Khaiary, Removal of basic dye from aqueous medium using a novel agricultural waste material: pumpkin seed hull, J. Hazard. Mater., 155 (2008) 601–609.